

Anode-Plasma Expansion in Pinch-Reflex Diodes

D. G. Colombant and Shyke A. Goldstein^(a)
Naval Research Laboratory, Washington, D. C. 20375
 (Received 8 June 1983)

Anode-plasma expansion in pinch-reflex diodes is investigated with use of a one-dimensional magnetohydrodynamic model. Early in time, the plasma undergoes thermal expansion and its front is slowed down as a result of $\vec{j} \times \vec{B}$. After the current has reached its maximum and for small radius where j and B are larger, $\vec{j} \times \vec{B}$ may accelerate the bulk of the anode plasma to large velocities. Good qualitative agreement is obtained with observations of the time dependence of the plasma velocity as well as its radial profile. The maximum expansion velocities reach tens of centimeters per microsecond.

PACS numbers: 52.25.Fi, 52.50.Dg, 84.70.+p

Anode-plasma dynamics is important in all pulsed-power ion diodes. In most diodes, it leads to anode-cathode gap closure and to the ion pulse termination. It may also have undesirable effects on ion beam brightness due to nonuniform anode plasma. Few studies,¹⁻⁴ experimental or theoretical, have been made of this critical phenomena. One study⁴ has determined some experimental characteristics of this expansion. First, large closure velocities up to 30 cm/ μ sec have been observed. Second, this large expansion is observed only late into the pulse (about 30 nsec into the ion pulse) and finally it takes place preferentially near the anode axis of symmetry. The 30 cm/ μ sec measured would correspond to a thermal expansion of a 0.4-keV CH₂ plasma which cannot be obtained by Ohmic heating alone for the measured plasma parameters. The two main theoretical attempts at explaining the anode plasma expansion have not been very conclusive. Nardi, Peleg, and Zinamon¹ have shown that 10-cm/ μ sec expansion takes place near the anode center because of the electron energy deposition in that region, but they did not reproduce the larger velocities observed nor the long delay in the expansion. Prono *et al.*² have studied a charge-exchange mechanism to account for the large expansion velocity but this mechanism does not explain the favored central expansion nor the large delay in the expansion. In the present work, we describe a model based on the dominant role played by the $\vec{j} \times \vec{B}$ force in the anode plasma expansion. In particular, the main results from this model are consistent with large final expansion velocities, with large expansion near the anode center, and with a long delay before fast expansion sets in.

The geometry of the model is shown in Fig. 1. The anode foil is planar and made of a nonconducting material (polyethylene). When electrons from the cathode accumulate on the anode surface,

flashovers occur and an anode plasma is formed just in front of the anode foil. This anode plasma serves as the source of the ions. When ions leave the plasma generating an ion current in the diode, the thermal electrons that are left behind flow radially inwards through the anode plasma where they are collected on a conducting rod at $r = r_{\min}$. The rest of the diode current flows from the cathode in the form of a relativistic electron beam (REB) which is assumed to pinch in vacuum from the diode radius R to a radius comparable to r_{\min} . For $z < 0$, all of the diode current is carried in the conducting rod and therefore, the magnetic field due to the total current develops behind the anode plasma. On the other hand, for $z > 0$, only a fraction of the total current contributes to the magnetic field. Because of that con-

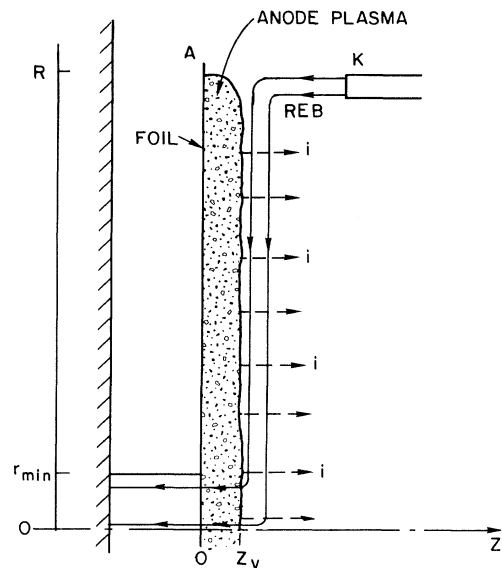


FIG. 1. Schematic of the anode-plasma model for pinch-reflex diode plasma expansion studied in the z direction as a function of radius. (A denotes the anode; K, the cathode.)

figuration, a gradient in magnetic pressure develops in the plasma. The force on the plasma due to this gradient is described by the local $\vec{j} \times \vec{B}$, where \vec{j} is due to the thermal electron current in the anode plasma. Notice that in the present model, the REB does not deposit its energy in the anode plasma but does contribute to the magnetic field there. The anode plasma is collision dominated and thus a fluid description is used to study its motion in the z direction. For simplicity, we have performed one-dimensional studies of the anode-plasma motion at various radii, approximating a two-dimensional picture by assuming that the thermal electron current has only a radial component.

The equations which describe the anode plasma are the magnetohydrodynamic equations⁵ which express conservation of mass, momentum, and energy. A magnetic diffusion equation closes the system. In the momentum equation, both thermal pressure gradient and $\vec{j} \times \vec{B}$ act on the plasma. In the energy equation, radiation losses have been neglected and the energy input into the plasma comes from the Ohmic heating term as well as $\vec{j} \times \vec{B}$ acceleration. The initial and boundary conditions which complete the set of assumptions are as follows. A low temperature is assumed for the C_2H_4 plasma at $t=0$ ($T \approx 0.5$ eV) as well as near-solid density ($n_i = n_{\text{solid}}/10$) which is assumed uniform over a thickness of 10^{-1} μm and corresponds roughly to an energy deposition⁶ of 0.1 J/cm². The electron and ion current waveforms are based on Ref. 4. The electron current starts 7 nsec before the ion current (at $t = -7$ nsec), rises linearly up to 925 kA in 37 nsec, and stays constant thereafter. The ion current rises linearly to 750 kA over 30 nsec and then remains constant. As for boundary conditions, the ion current density j_z for $z > z_v$, where z_v denotes the plasma-beam interface, is assumed to be inversely proportional to r . This relationship has been demonstrated both experimentally⁷ and in particle simulation.⁸ The resulting B field at $z = z_v$ due to the ion current is independent of radius. The B field due to the REB current is inversely proportional to r for $z=0$ and $z=z_v$. Because of the time dependence of the currents, the B field increases with time both at $z=0$ and $z=z_v$ and is larger at $z=0$. The boundary condition to determine the position of z_v follows from both plasma expansion and plasma erosion. The expansion is determined simply by the plasma boundary velocity $v_p(z_v)$. The anode-plasma erosion is due to the ion-beam extraction by the di-

ode electric field at $z > z_v$ which prevents plasma electrons from following the ions. The expression for z_v is then $v_F = dz_v/dt = v_p(z_v) - j_i/en_i$, where the subscript i refers to the ions. From that expression, and for typical peak parameters, $j_i = 100$ kA/cm², $v_p \approx 10^7$ cm/sec, the plasma number density at z_v is $n_i \approx 10^{17}$ cm⁻³ or $\rho \approx 10^{-6}$ g/cm³ for a CH_2 plasma.

Other features of the model concern its treatment of the equation of state and of the electrical resistivity. The equation of states for CH_2 was taken from standard SESAME tables⁹ except that at low temperatures and high density, corrections were made to take into account the fact that C_2H_4 dissociated into CH_2 , and then into $C + H + H$. Electrical resistivity was assumed to be classical and was supplemented by electron-neutral collision resistivity at low temperatures and by anomalous resistivity at high temperature and low density. The anomalous resistivity was required only late into the pulse, on the anode side as will be discussed later.

Results were obtained for $I_{i \text{ max}} \approx I_{e \text{ max}} \approx 750$ kA, τ_p (linear ramp) = 30 nsec, $R = 5$ cm, and initial plasma mass density per unit area = 3.5×10^{-6} g/cm². Plasma expansion was calculated for the different radii $r = 1, 2.5,$ and 4 cm. The following is a brief summary and analysis of the results. In all cases, pressure gradients dominated the $\vec{j} \times \vec{B}$ force in the first few nanoseconds and gave rise to expansion velocities of a few times the thermal sound speed or a few centimeters per microsecond.

When the $\vec{j} \times \vec{B}$ force becomes important, it first has the effect of slowing down the plasma in the vicinity of z_v . In order to explain that effect, we use as an example the information in Fig. 2 where density, velocity, B field, and current density profiles are shown as a function of z at $t = 14$ nsec and $r = 1$ cm. The main feature of the B -field profile in Fig. 2(a) is the dip inside the plasma. Because $j_r = -(c/4\pi)\partial B/\partial z$, we see that for $z < z_d$ $\vec{j} \times \vec{B}$ accelerates the plasma outwards whereas for $z > z_d$, $\vec{j} \times \vec{B}$ slows down the plasma. The reasons for this dip are the following: near $z=0$, the plasma density is very high, the temperature rises very slowly, and the magnetic field diffuses rapidly through the plasma as shown by the B -field plateau. For $z \lesssim z_v$ on the other hand, the plasma density is low, its temperature is high, and it expands in the axial direction. This expansion reduces the magnetic field inside the plasma, slowing down the diffusion process which is already weaker than on the low-tempera-

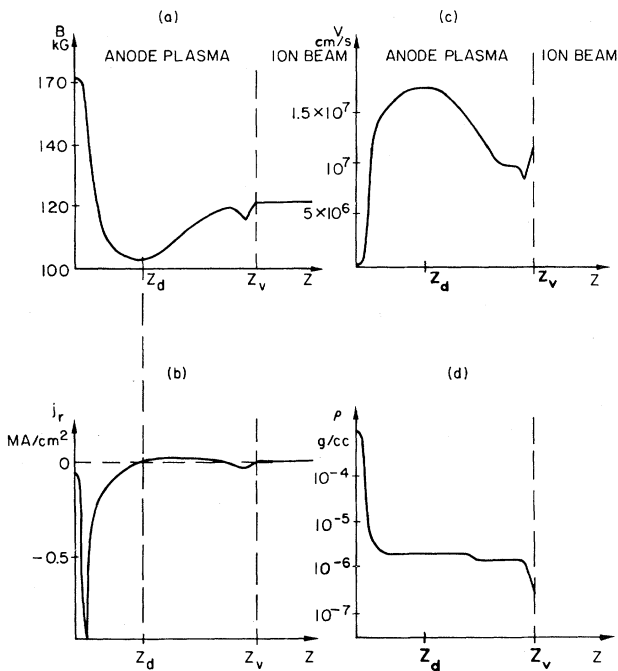


FIG. 2. Typical B field, plasma current density, axial velocity, and mass density profiles as a function of distance along axis. Note that the origin in z corresponds to the cathode side of the anode foil. Profiles are shown at $t = 14$ nsec for $r = 1$ cm.

ture side (at $z \approx 0$). The ensuing confinement effect for $z_d < z < z_v$ is seen on the velocity and density profiles in Figs. 2(c) and 2(d). The density profile in Fig. 2(d) stays nearly constant because of the slowing down effect of $\vec{j} \times \vec{B}$ in the above domain. When the $\vec{j} \times \vec{B}$ force was artificially suppressed in the calculations, no density plateau was observed.

As time increases, $\vec{j} \times \vec{B}$ may be large enough so that the velocity profile between z_d (higher velocity) and z_v (lower velocity) changes significantly. In that case, the distance $z_v - z_d$ will shrink during the duration of the ion beam pulse. The front velocity v_F will then exhibit a sudden change in value from $v(z_v)$ to $v(z_d)$ as $z_v - z_d$ goes to zero. The whole anode plasma at $z \leq z_d$ is accelerated during that time, reaching velocities of tens of centimeters per microsecond. This situation occurs especially at small radii where both j and B are larger. For the case of Fig. 2, the velocity $v_p(z_d)$ remains approximately constant at $16 \text{ cm}/\mu\text{sec}$ from 10 to 30 nsec whereas $v_p(z_v)$ gradually decreases from 12 to $5 \text{ cm}/\mu\text{sec}$. Later in the pulse, as $z_v - z_d$ approaches zero, the plasma moves at velocities up to $30 \text{ cm}/\mu\text{sec}$ at

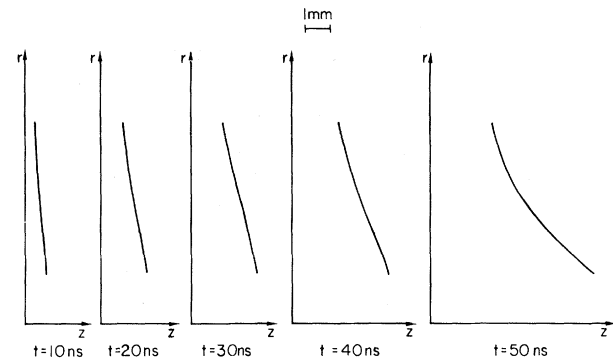


FIG. 3. Position of the anode-plasma front (defined by z_v) as a function of time. Calculations have been made at three different radii.

$t = 50$ nsec. At large radii, however, $\vec{j} \times \vec{B}$ is smaller and does not generate a velocity differential between z_d and z_v large enough to cause complete shrinkage of this gap. The plasma front velocity v_F is nearly equal to $10 \text{ cm}/\mu\text{sec}$ and does not undergo any abrupt changes. The plasma front location as a function of radius is shown in Fig. 3 at various times. We see that the experimental observations of large velocities late in the pulse as well as the larger acceleration near the anode center are all in qualitative agreement with the results of the present model. The results of the present model have been checked for their sensitivity to the following variations.

Initial plasma mass.—The mass was changed from $3.5 \times 10^{-6} \text{ g}/\text{cm}^2$ to $8.5 \times 10^{-6} \text{ g}/\text{cm}^2$ for $r = 1$ cm while keeping the same initial density gradient. The thermal expansion in the early stages is very similar and results in the same value for the front velocity. Then, in both cases, the current density peaks at the foot of the density gradient and gradually erodes it. In time, this plasma expands and as mentioned previously is slowed down by the $\vec{j} \times \vec{B}$ force. Up to times of 30 nsec, there are no major differences between the two mass-density cases. However, later in the pulse, the reduction in density near $z = 0$ for the more massive target is slower and once the plasma starts to be accelerated from the back, it reaches lower velocities since there is more of it. An integral of the momentum equation gives the average velocity in the later stages when the total pressure differential across the plasma can be neglected, $\langle v \rangle = I^2 t_{\text{acc}} / 200 \pi m_0 r^2$, where t_{acc} is the time over which acceleration from the back takes place. This equation also gives a very rough check on the code (because of the assumption on

the pressure differential). For example, for the case of Fig. 2, we find that for $I \approx 1.5$ MA, $t_{\text{acc}} = 25$ nsec, $r = 1$ cm, and $m_0 = 3.5 \times 10^{-6}$ g/cm², then $\langle v \rangle = 26$ cm/ μ sec, whereas the code gives 23 cm/ μ sec at $t = 50$ nsec. For $m_0 = 8.5 \times 10^{-6}$ g/cm², the observed pressure differential is not negligible and we find that $\langle v \rangle = 10.7$ cm/ μ sec whereas the code gives 15 cm/ μ sec at $t = 50$ nsec.

Maximum temperature in the low-density plasma.—A low-density plasma ($\rho \lesssim 10^{-7}$ g/cm³) may be present in the calculations at both boundaries, on the cathode side naturally and on the anode side late in the pulse when the whole plasma is being pushed from behind by the $\vec{j} \times \vec{B}$ force. If current is still allowed to flow in this region, the temperature can reach several kiloelectronvolts. Because of the low plasma density ($n_e \approx 10^{15}$ cm⁻³) and the high current density [$j \approx 10^6$ A/cm², see Fig. 2(b)] on the anode side (near $z = 0$), the drift velocity ($V_D \sim 5 \times 10^9$ cm/sec) exceeds the thermal velocity for the electrons and the plasma becomes anomalously resistive. In order to avoid such excessive heating, a simple anomalous resistivity model was used and a temperature limit was also imposed in that region. The present results were obtained for $T \leq 200$ eV. This limit affects only the results for the lower-mass-density case at $r = 1$ cm. For all the other cases, the temperature did not reach 100 eV in that region (either because of the larger mass or the lower current).

In conclusion, it has been shown for the first time that anode-plasma expansion can be explained in terms of a magnetohydrodynamic model and that the main observations of the time history of the expansion, large final velocities (30 cm/ μ sec), and preferred acceleration near the anode center are well reproduced by the model. Improvements to the present model should include a detailed treatment of the resistivity in the low-density regions ($n_e \lesssim 10^{15}$ cm⁻³) as well as a two-

temperature model. The important implication of this work for plasma diodes is that there is a limit on how small high-power diodes can be made and how short the pulse length should be before running into limitations due to anode-plasma expansion. Other diodes besides the pinch-reflex diode should also be investigated in that respect with use of models similar to the one presented here.

This work was supported by the U. S. Department of Energy.

^(a)Permanent address: Jaycor, Alexandria, Va. 22304.

¹E. Nardi, E. Peleg, and Z. Zinamon, *Plasma Phys.* **20**, 597 (1978).

²D. S. Prono, H. Ishizuka, E. P. Lee, B. W. Stallard, and W. C. Turner, *J. Appl. Phys.* **52**, 3004 (1981).

³S. A. Goldstein, D. W. Swain, G. R. Hadley, and L. P. Mix, in *Proceedings of the International Topical Conference on Electron Beam Research and Technology, Albuquerque, 1975*, edited by G. Yonas (Sandia Laboratory, Albuquerque, 1976), p. 262.

⁴J. W. Maenchen, F. C. Young, R. Stringfield, S. J. Stephanakis, D. Mosher, Shyke A. Goldstein, R. D. Guenario, and G. Cooperstein, *J. Appl. Phys.* **54**, 89 (1983).

⁵S. I. Braginskii, in *Reviews of Plasma Physics*, edited by M. A. Leontovich (Consultants Bureau, New York, 1965), Vol. I., p. 262.

⁶S. Humphries, Jr., *Nucl. Fusion* **20**, 1549 (1980).

⁷A. E. Blaugrund, S. J. Stephanakis, and Shyke A. Goldstein, *J. Appl. Phys.* **53**, 7280 (1982).

⁸A. T. Drobot, R. J. Barker, R. Lee, A. Sternlieb, D. Mosher, and Shyke A. Goldstein, in *Proceedings of the Third International Conference on High Power Electron and Ion Beam Research and Technology, Novosibirsk, July 1979* (Institute of Nuclear Physics, Novosibirsk, 1979), p. 647.

⁹D. I. Bennett, J. B. Johnson, G. I. Kerley, and G. T. Rood, Los Alamos Scientific Laboratory Report No. LA 7130, 1978 (unpublished).